Am J Transl Res 2025;17(12):9290-9303
www.ajtr.org /ISSN:1943-8141/AJTR0167469

Original Article

MiR-183-5p modulates inflammatory response and apoptosis in diabetic nephropathy by targeting the TTP

Ziqi Li, Yan Wang, Yan Gu

Department of Geriatric Medicine, Nantong First People's Hospital, Nantong 226000, Jiangsu, China

Received July 15, 2025; Accepted November 24, 2025; Epub December 15, 2025; Published December 30, 2025

Abstract: Objective: To clarify the involvement of miR-183-5p, tristetraprolin (TTP), and inflammatory cytokines in Diabetic nephropathy (DN). Methods: This retrospective study included 10 patients with DN, 10 patients with type 2 diabetes (T2DM) and 10 controls. Expression levels of miR-183-5p and TTP in T2DM patients and DN patients were detected, and the correlation between miR-183-5p, TTP, and inflammatory cytokines were analyzed. Renal tubular epithelial cells (HK-2) served as the cell model. The expression of TTP and cytokines in the cell cultures was detected using qRT-PCR or ELISA. Results: miR-183-5p promoted inflammation and apoptosis in the context of hyperglycemia. TTP was identified as the direct target of miR-183-5p. Elevated miR-183-5p expression in HK-2 cells resulted in increased inflammatory cytokine release and enhanced apoptosis. miR-183-5p inhibitors significantly reduced the levels of inflammatory cytokines in HK-2 cells. Conclusions: MiR-183-5p accelerates DN development through its action on TTP, thereby presenting a new therapeutic avenue for DN.

Keywords: MiR-183-5p, apoptosis, diabetic nephropathy, tristetraprolin

Introduction

Diabetic nephropathy (DN) is the most common microvascular complication of diabetes and a leading cause of chronic complication-associated mortality in diabetic patients [1-3]. Its clinical manifestations include proteinuria, edema, hypertension, and progressive deterioration of renal function. DN plays a crucial role in driving the progression of end-stage renal disease (ESRD), which is rising annually [4, 5]. Currently, no specific treatment exists for DN, and patients generally have poor clinical outcomes. Consequently, identifying biomarkers and effective targets for early diagnosis are particularly important. Although the underlying mechanisms remain incompletely understood, recent studies have shown that multiple microRNAs (miRNAs) exhibit abnormal expression in DN patients and participate in ND processes, such as mesangial extracellular matrix (ECM) accumulation and podocyte injury [6-8]. Therefore, miRNA-based research may offer novel insights for clinical management of DN.

MiRNAs are short RNA sequences approximately 19 to 25 nucleotides in length, derived from endogenous genes and widely present in eukaryotes and viruses [9, 10]. Each miRNA can regulate multiple genes, while multiple miRNAs can collectively regulate the same genes. MiRNAs bind to and active the RNA-induced silencing complex (RISC). Studies have confirmed that miRNAs participate in various pathological processes of DN through different mechanisms. MiRNAs are associated with hemodynamic changes in DN [11], regulate cell cycle [12], and contribute to inflammatory and immune responses. Evidence suggests that under hyperglycemic conditions, the upregulation of some miRNAs, such as miRNA-146a, can directly inhibit their target genes - TNF Receptor-Associated Factor 6 (TRAF6) and Interleukin-1 Receptor-Associated Kinase 1 (IRAK1) - thus inhibiting inflammatory response in DN [6, 13]. Therefore, by acting on target genes to suppress inflammatory responses, miRNAs may exert beneficial effects during the early stages of DN.

Zinc finger protein-36 (ZFP36) gene encodes tristetraprolin (TTP), an RNA-binding protein capable of binding to the ARE region of multiple target gene mRNAs to promote their degrada-

https://doi.org/10.62347/MIIS3722

tion. TTP is expressed at low levels in a variety of cells, and its overexpression can be induced by factors such as phobosyl, insulin, mitogen and apolipoprotein. Studies have shown that multiple intracellular signaling pathways regulate TTP expression, phosphorylation, subcellular localization, and interaction with other proteins, and these processes are crucial for pathological progression of inflammation and malignancies [14, 15]. However, few reports exist on the correlation between TTP and clinical factors or biochemical indicators in DN patients. This study aims to investigate the effects of miR-183-5p on TTP regulation and inflammatory cytokine levels in DN patients, elucidate the interaction between miR-183-5p and TTP, and clarify their role in DN pathogenesis.

Materials and methods

Patient information and sample collection

Blood samples were collected from 10 healthy volunteers, 10 patients with type 2 diabetes mellitus (T2DM), and 10 DN patients at Nantong First People's Hospital. The healthy control group comprised individuals with normal blood pressure and no history of diabetes, kidney disease or other severe illness. There were no statistically significant differences in age or gender distribution among the study groups. All subjects underwent rigorous screening to ensure the absence of acute infections, autoimmune diseases, malignancies, or other severe chronic conditions that could substantially influence miRNA expression profiles. This retrospective study was approved by the Ethics Committee of Nantong First People's Hospital, covering all tissue specimen collection and experimental protocols.

Cell culture and transfection

HK-2 cells and human renal glomerular mesangial cells (HRGMCs) were purchased from the American Type Culture Collection (ATCC, Manassas, VA, USA). Cells were cultured in RPMI 1640 medium supplemented with 10% fetal bovine serum (Gibco, Life Technologies) and 1% penicillin/streptomycin (Hycult, Life Technologies). Cells were maintained in a constant-temperature sterile incubator at 37°C with 5% CO_2 and digested with 0.25% trypsin. The TTP-overexpressed plasmid, validated by transfection and sequencing, underwent monoclonal amplification after successful sequencing. DNA extraction was performed per kit instructions, with concentration determined. Following the plasmid transfection reagent manual, the TTP-overexpressed plasmid was transfected into the cells in the logarithmic growth phase, and corresponding unloaded control groups were established. Medium was changed 5 hours after transfection, and the protein and RNA were extracted every 24 hours to verify the expression of relevant target genes and proceed with subsequent experiments. MiR-183-5p mimics and negative controls were transfected into HK-2 cells at a concentration of 50 nmol/L. After 24 hours of transfection, cell samples were collected for biological assays. To establish a hyperglycemic stimulation model, standard concentration of glucose (5.5 mM), high concentration glucose (25 nM), and high concentration mannitol (25 nM) were added to the renal tubular epithelial HK-2 cells.

ELISA assay

Interleukin (IL)-6 and tumor necrosis factor-alpha (TNF-α) levels were measured utilizing IL-6 and TNF-α ELISA kit (Elascience, Wuhan, China). Absorbance at 450 nm wavelength was measured using an ELISA reader (MultiskanEX, Lab systems, Helsinki, Finland). Each experiment was repeated five times, and the mean value was recorded. Creatinine (Cr), blood urea nitrogen (BUN), hemoglobin A1c (HbA1c), triglyceride (TG), and albumin were determined using an automatic biochemical analyzer (CS400, Changchun Dirui Medical Technology Co., Ltd., Changchun, China).

MTT assay

Cells at the logarithmic phase were seeded at a density of 3.0×10^4 cells/mL into a 96-well plate, with 100 μL per well. After cell attachment, each well was processed according to experimental groups. After 72 h of incubation, 20 μL MTT (5 mg/mL) (Beyotime, Shanghai, China) was added to each well, followed by additional 4 h incubation. Then, the supernatant was aspirated, followed by addition of 150 ml DMSO into each well. After rapid dissolution, the absorbance value at 490 nm wavelength was measured (MultiskanEX, Lab systems, Helsinki, Finland).

Table 1. The primers used for real-time PCR

Target gene	Forward sequence (5' to 3')	Reverse sequence (5' to 3')
TTP	CTTTCCCCTTCTGCCTTCTC	TGGTGCTGGGGGTAGTAGAC
IL-6	CCGGAGAGGAGACTTCACAG	CAGAATTGCCATTGCACAAC
TNF-α	GCTGAGCTCAAACCCTGGTA	CGGACTCCGCAAAGTCTAAG
GAPDH	AGAACATCATCCCTGCATCC	CACATTGGGGGTAGGAACAC
U6	ATTGGAACGATACAGAGAAGATT	GGAACGCTTCACGAATTTG

TTP: tristetraprolin; IL-6: interleukin-6; TNF-α: tumor necrosis factor-alpha.

Flow cytometry

Three replicates were established for each group. Cells were collected after 48 h and 72 h of trypsin digestion. The cells were resuspended in 250 μL binding buffer at a concentration of 1×10^5 cells/mL. Five μL Annexin-V-FITC and 5 μL propidium iodide (PI) (Beyotime, Shanghai, China) were sequentially added to the resuspension, followed by incubation on ice for 15 min in the dark. Four hundred μL refresh mixed buffer was added and mixed thoroughly. Quantitative analysis was performed using a flow cytometer (Partec CyFlow Space, Münster, Germany) and FlowJo software (Tree Star, Ashland, OR, USA). Each experiment was repeated in triplicate.

TUNEL assay

Following fixation, cells in each group were processed according to the TUNEL kit protocol (Beyotime, Shanghai, China). A 0.1% citric solution containing 0.1% Tween X-100 was added and incubated on ice for 3 min. Then, 50 μL TUNEL reaction solution was added to each sample, placed in a humidified chamber, and incubated at 37°C for 1 h. Subsequently, 100 μg/L DAPI nuclear stain was added and incubated for 8 min. The field film was captured using a fluorescence microscope (OLYMPUS, BX51TF type). Apoptotic nuclei appeared green, and apoptotic cells were counted by a pathologist that blinded to the grouping. Five random fields per section were counted.

qRT-PCR

RNA was isolated and purified using Takara total RNA extraction kit (Invitrogen, Carlsbad, CA, USA), and the RNA concentration was measured. RNA was converted to cDNA using the Takara Reverse Transcription Kit (Invitrogen, Carlsbad, CA, USA), followed by staining and fluorescence quantitative real-time PCR. Primer sequences are listed in **Table 1**. GAPDH served as the internal reference. Relative quantification was performed using the $2^{-\Delta\Delta Ct}$ method. ABI PRISM 7300 sequence detection system (Applied Biosystems, Foster City, CA, USA) was applied to quantify gene expression. Three sub-holes were set in each group, and the procedure was performed three times.

Dual luciferase reporter gene assay

TTP was identified as a target of miR-183-5p via TargetScan analysis. TTP mRNA 3'-UTR fragments containing the miR-183-5p target site and TTP 3'-UTR fragments with target site mutations were inserted into a reporter vector (designed by Shanghai Jima Biotechnology Co., Ltd.). Cells were harvested during the exponential growth phase and seeded into 6-well plates at a density of 1×10^6/cells/well. Upon reaching 90% confluency, cells were transfected with miR-183-5p mimics using Lipofectamine™2000 (Invitrogen, Carlsbad, CA, USA) according to manufacturer's instructions. After 24 h of simultaneous transfection, the relative luciferase activity was measured and analyzed according to the guidelines of the dual-luciferase reporter assay system.

RNA pull-down

RNA sequences containing biotin were digested with RNase-free DNaseI and then purified using the RNeasy MiniKit (Invitrogen, Carlsbad, CA, USA). One μg of labeled RNA was placed in RNA structure buffer (10 mmol/L, TrispH7, 0.1 mol/L, KCl, 10 mmol/L, $MgCl_2$). This was heated at 95°C for 2 minutes, and incubated on ice for 3 min. The solution was maintained at room temperature for 30 min to allow RNA to form appropriate secondary structures. For cell lysate extraction, 400 ng labeled RNA and 500 μL RIP buffer were added into the centrifuge tube, and incubated at standard temperature for 1 h. Then, 50 μL streptavidin agarose arose beads were added, followed by incubation for 1 h. Washing occurred five times with RIP buffer, and samples were collected for RT-PCR detection.

Animal models and experimental design

Male db/db mice and their age-matched lean control db/+ littermates were purchased from Wuhan Experimental Animal Center, all aged 6 weeks. Mice were housed under specific pathogen-free conditions with a 12-hour light/dark cycle, provided with standard chow and ad libitum water. At 8 weeks of age, db/db mice were randomly assigned into three groups (n = 5 per group): db/db control group, db/db+ NC inhibitor group (tail-vein injection, 5 nmol), and db/db+miR-183-5p inhibitor group (tail-vein injection, 5 nmol). The inhibitors were dissolved in sterile phosphate-buffered saline (PBS) and administered weekly for 4 weeks. The db/+ control mice received PBS injections as vehicle controls. Mice were euthanized by gradual CO_2 exposure at a rate of 20% of the cage volume per minute. Respiratory cessation was confirmed, followed by cervical dislocation as a secondary confirmation method to ensure animal death. All experimental procedures were approved by the Institutional Animal Care and Use Committee and conducted in accordance with the Guidelines for the Care and Use of Laboratory Animals.

Statistical analysis

Statistical analysis was conducted using SPSS 17.0 (SPSS Inc., Chicago, IL, USA) and GraphPad Prism 6 software (GraphPad Software, Inc., San Diego, CA, USA). Data were expressed as mean ± standard deviation. Multiple group comparison was conducted using one-way ANOVA, while pair-wise comparison was performed using a t-test. $P < 0.05$ was considered statistically significant.

Results

The clinical indexes of healthy controls, diabetic patients and diabetic nephropathy patients were analyzed

Blood samples were collected from 10 healthy volunteers, 10 participants with T2DM, and 10 DN patients. Changes in multiple indicators were analyzed. The results revealed that, compared with the healthy control group, both the T2DM group and DN group demonstrated significantly higher levels of TG, TA and UA, with higher levels in DN patients (**Figure 1A-C**). No significant differences were observed in BUN and Cr levels between the control group and T2DM group; however, the DN group showed significantly higher BUN and Cr compared with the other two groups (**Figure 1D**, **1E**). HbA1c was significantly elevated in the T2DM and DN group compared with the control group, but with no significant difference between T2DM and DN groups (**Figure 1F**). UAER was notably higher in the DN group compared with the control and T2DM groups (**Figure 1G**).

Serum expression of TTP, miR-183-5p, and inflammatory markers in the three groups

The expression of miR-183-5p was significantly elevated in the T2DM and DN groups compared to the control group, with the level being significantly higher in the DN group than the T2DM group (**Figure 2A**). In contrast, the expression trend of TTP was opposite to that of miR-183-5p, with TTP markedly decreased in the T2DM and DN group (**Figure 2B**). In terms of inflammatory markers, the DN group showed significantly elevated expression of TNF-α and IL-6 compared to the Control group and the T2DM group (**Figure 2C**, **2D**). A positive correlation was observed between miR-183-5p expression and inflammatory factors (IL-6 and TNF-α) (**Figure 2E**, **2F**).

Expression patterns of TTP, miR-183-5p, and inflammatory markers in HK-2 cells exposed to high glucose

As previously mentioned, plasma levels of miR-183-5p in patients with DN were different from those in the NC and T2DM groups. In this study, renal tubular epithelial cells (HK-2 cells) were cultured with high glucose, and the expression of miR-183-5p was measured. After high glucose stimulation, the levels of miR-183-5p were markedly elevated, while no such effect was observed with mannitol treatment (**Figure 3A**). qPCR results demonstrated that TTP expression was notably downregulated in response to high glucose (**Figure 3B**). Further, analysis of inflammatory markers showed that high glucose stimulation significantly increased IL-6 and TNF-α expression (**Figure 3C**, **3D**). Overall, miR-183-5p and inflammatory cytokines are elevated under hyperglycemic conditions, while TTP expression is decreased, suggesting the involvement of miR-183-5p and TTP in the inflammatory process under hyperglycemia.

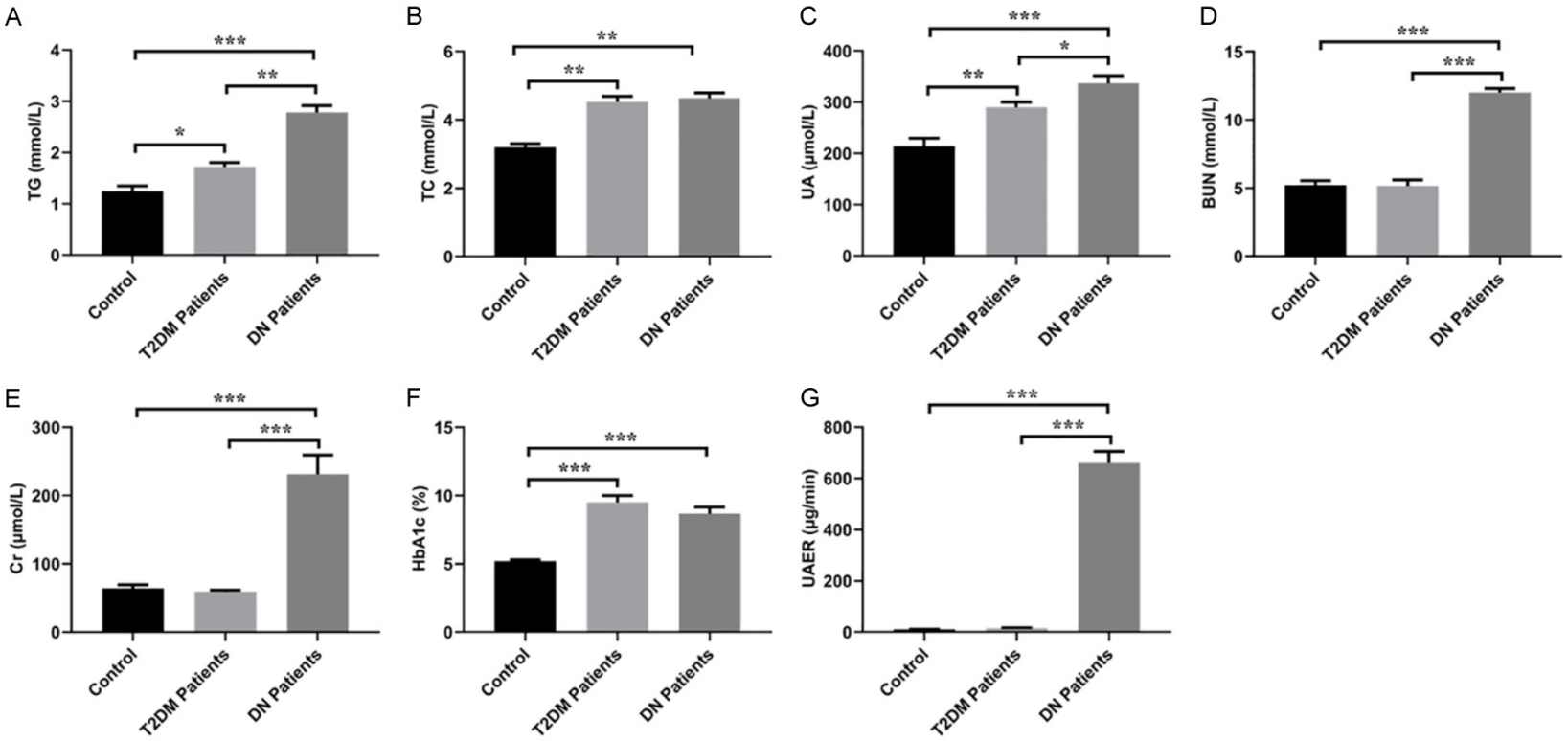

Figure 1. Comparison of laboratory parameters among control group, T2DM group and DN group. A. TG; B. TC; C. UA; D. BUN; E. Cr; F. HBA1c; G. UAER. *P < 0.05, **P < 0.01, ***P < 0.001. T2DM: type 2 diabetes mellitus, DN: diabetic nephropathy, TG: triglyceride, TC: serum total cholesterol, UA: uric acid, BUN, blood urea nitrogen, Cr: serum creatinine, HbA1c: Glycated hemoglobin, UAER: urinary albumin excretion rates.

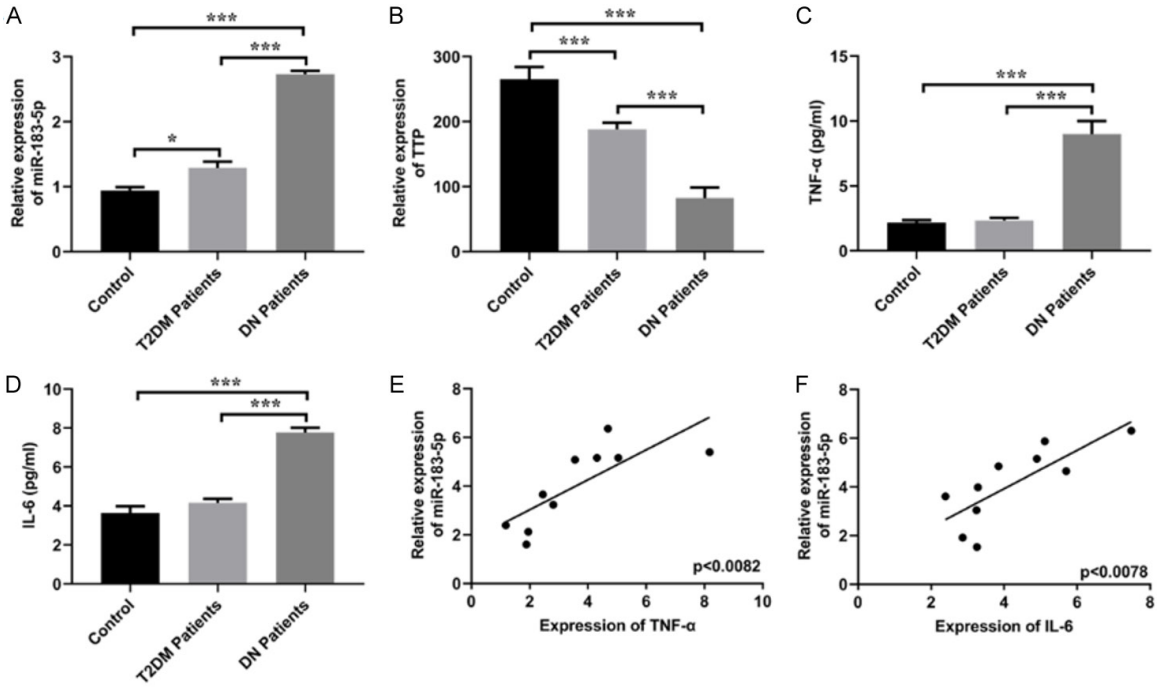

Figure 2. Expression of miR-183-5p, TTP, and inflammatory factors in three groups. A. Comparison of serum miR-183-5p level among the three groups; B. Comparison of serum TTP level among the three groups; C. Comparison of serum TNF-α levels among three groups; D. Comparison of serum IL-6 levels among three groups; E. Correlation analysis between miR-183-5p and IL-6; F. Correlation analysis between miR-183-5p and TNF-α. ***P < 0.001. TTP: tristetraprolin; IL-6: interleukin-6; TNF-α: tumor necrosis factor-alpha.

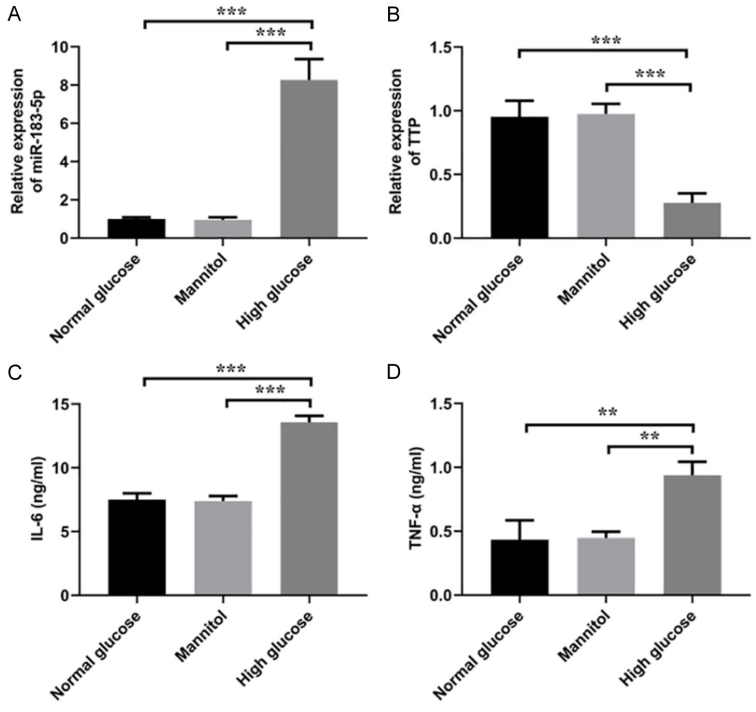

Figure 3. Expression of miR-183-5p, TTP, and inflammatory factors in HK-2 cells under high glucose condition. A. miR-183-5p expression; B. TTP expression; C. IL-6 expression; D. TNF-α expression. **P < 0.01, ***P < 0.001. TTP: tristetraprolin; IL-6: interleukin-6; TNF-α: tumor necrosis factor-alpha.

Inhibition of miR-183-5p reduced hyperglycemic-induced inflammation and apoptosis

To further investigate the regulatory effect of miR-183-5p on TTP, HK-2 cells were treated with a miR-183-5p inhibitor followed by high glucose (HG) exposure. The findings showed that HG up-regulated miR-183-5p levels, while the miR-183-5p inhibitor effectively inhibited miR-183-5p levels (**Figure 4A**). MTT assay indicated that HG exposure suppressed HK-2 cell proliferation, which was restored by miR-183-5p inhibitor (**Figure 4B**). Findings from IL-6 and TNF-α expression tests showed that HG exposure upregulated the levels of IL-6 and TNF-α, which was reversed by miR-183-5p inhibitor (**Figure 4C**, **4D**).

Flow cytometry results showed that HG exposure promoted

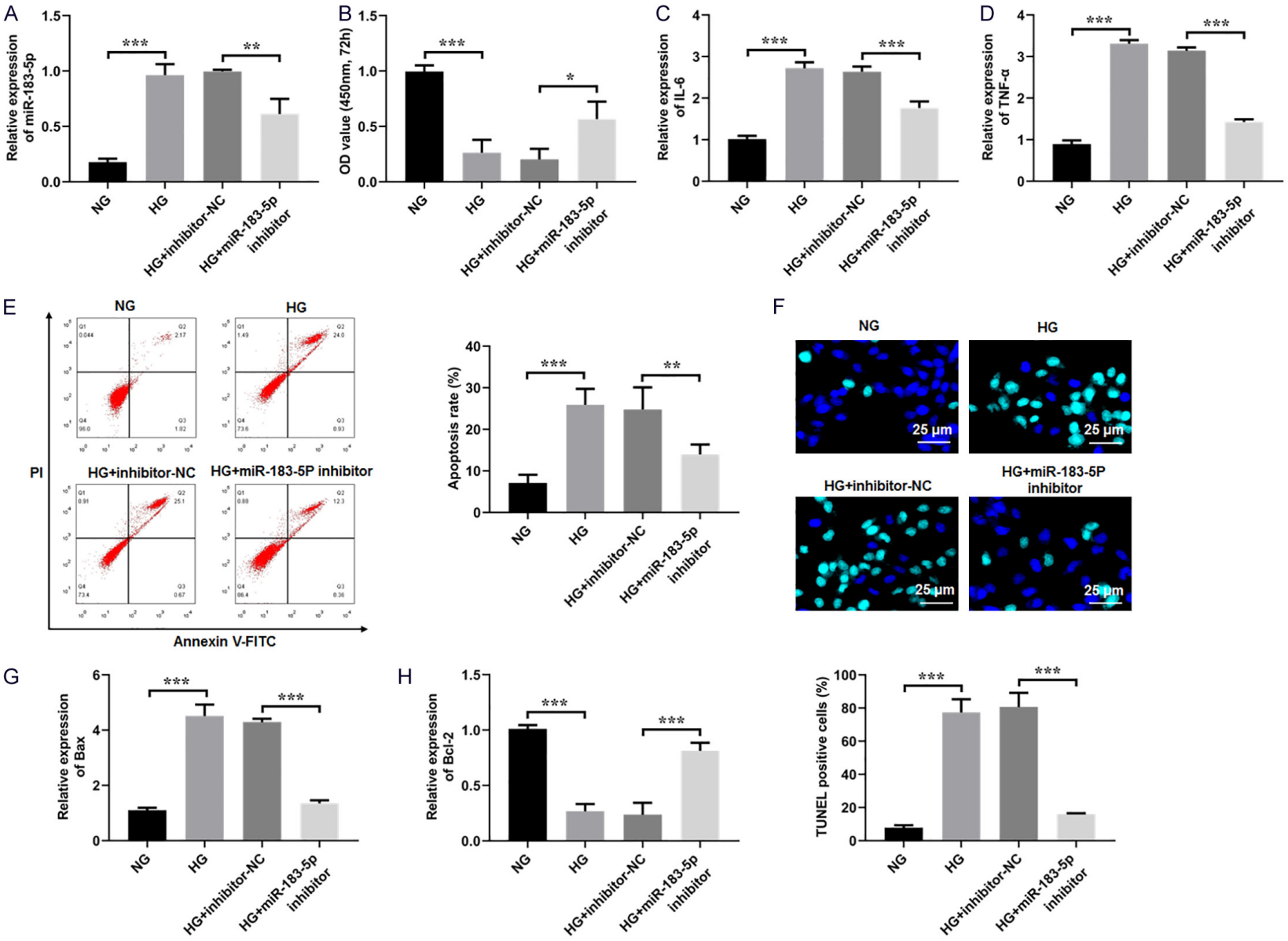

Figure 4. Inhibition of miR-183-5p reduced hyperglycemia-induced inflammation and apoptosis. A. miR-183-5p expression detected under different treatment; B. Cell proliferation measured after various treatments; C. IL-6 expression assessed following different treatments; D. TNF-α expression assessed following different

treatments; E. Apoptosis detected by flow cytometry after different treatments; F. Apoptosis detected by TUNEL after different treatments. Scale = 25 μm. G. Bax expression assessed after different treatments; H. Bcl-2 expression assessed after different treatments. **P < 0.01, ***P < 0.001. IL-6: interleukin-6; TNF-α: tumor necrosis factor-alpha; Bax: Bcl-2-associated X protein; Bcl-2: B-cell lymphoma 2.

HK-2 cell apoptosis, and miR-183-5p inhibitor significantly reduced the apoptosis rate (**Figure 4E**). The findings from TUNEL apoptosis were consistent with those from flow cytometry. The content of TUNEL positive HK-2 cells significantly increased after HG induction, while miR-183-5p inhibitor reduced HG-induced apoptosis (**Figure 4F**). Further detection of apoptosis-related proteins showed that HG induction significantly up-regulated the level of Bax but reduced the level of Bcl-2, which were reversed by miR-183-5p inhibitor (**Figure 4G**, **4H**). In HG-treated HRGMCs, miR-183-5p expression was significantly upregulated, while transfection with miR-183-5p inhibitor effectively reduced miR-183-5p expression (Supplementary Figure 1A). Additionally, HG treatment increased TNF-α secretion (Supplementary Figure 1B), upregulated the pro-apoptotic protein Bax (Supplementary Figure 1C), and induced apoptosis (Supplementary Figure 1D). Notably, inhibition of miR-183-5p markedly attenuated these HG-induced inflammatory and apoptotic responses.

To further confirm whether the effects brought by HG treatment were caused by the metabolic action of glucose or merely due to the non-specific stress response resulting from increased osmotic pressure, we added the mannitol osmotic control group (5.5 mM glucose +19.5 mM mannitol) and detected the levels of cell inflammation and apoptosis. Our results show that inflammatory markers and apoptosis were significantly higher in the HG group compared to both NG and MG groups, while the MG group shows only mild changes, suggesting that the observed effects were primarily driven by high glucose metabolism rather than osmotic stress (Supplementary Figure 2).

TTP was identified as a target gene of miR-183-5p

Subsequently, we started to identify the potential target of miR-183-5p under hyperglycemic conditions. Through TargetScan analysis, we determined that TTP is a potential target of miR-183-5p. Results revealed a highly conserved miR-183-5p binding site within the 3'-UTR region of TTP (**Figure 5A**). To examine whether the binding of miR-183-5p to TTP mRNA resulted in translational inhibition, we cloned the 3'-UTR of TTP into the luciferase reporter vector pmirGLO and simultaneously constructed a mutant. In renal tubular epithelial cells, transient co-transfection of miR-183-5p with wild-type (WT) TTP 3'-UTR significantly inhibited luciferase reporter expression; however, mutations of the TTP binding site abolished this inhibition (**Figure 5B**). These outcomes collectively indicate that miR-183-5p directly interacts with TTP by binding its 3'-UTR region and suppresses its function.

To further validate miR-183-5p's targeting of TTP, we introduced miR-183-5p mimics or inhibitors into HK-2 cells. Results confirmed that miR-183-5p mimic promoted miR-183-5p expression and suppressed TTP mRNA and protein expression, while miR-183-5p inhibitor reduced miR-183-5p expression (**Figure 5C**) and promoted mRNA and protein expression of TTP (**Figure 5D**, **5E**). Next, RNA precipitation (**Figure 5F**) and RNA immunoprecipitation (**Figure 5G**) experiments further validated the targeting of miR-183-5p to the TTP 3'-UTR. The correlation analysis revealed a negative correlation between miR-183-5p and TTP (**Figure 5H**).

In HG-treated HRGMCs, overexpression of miR-183-5p suppressed TTP expression, and this effect was reversed by co-transfection with a TTP overexpression plasmid (Supplementary Figure 3A). Furthermore, when the TTP overexpression plasmid was co-transfected with the miR-183-5p mimic into HG-treated cells, the promoting effects of the miR-183-5p mimic on TNF-α secretion (Supplementary Figure 3B), Bax expression (Supplementary Figure 3C), and apoptosis (Supplementary Figure 3D) were abolished. These findings indicate that miR-183-5p promotes HG-induced inflammatory response and apoptosis by directly targeting and suppressing TTP expression.

TTP overexpression reversed the pro-inflammatory effects of miR-183-5p and attenuated apoptosis

To validate the association between TTP and miR-183-5p in DN progression and elucidate

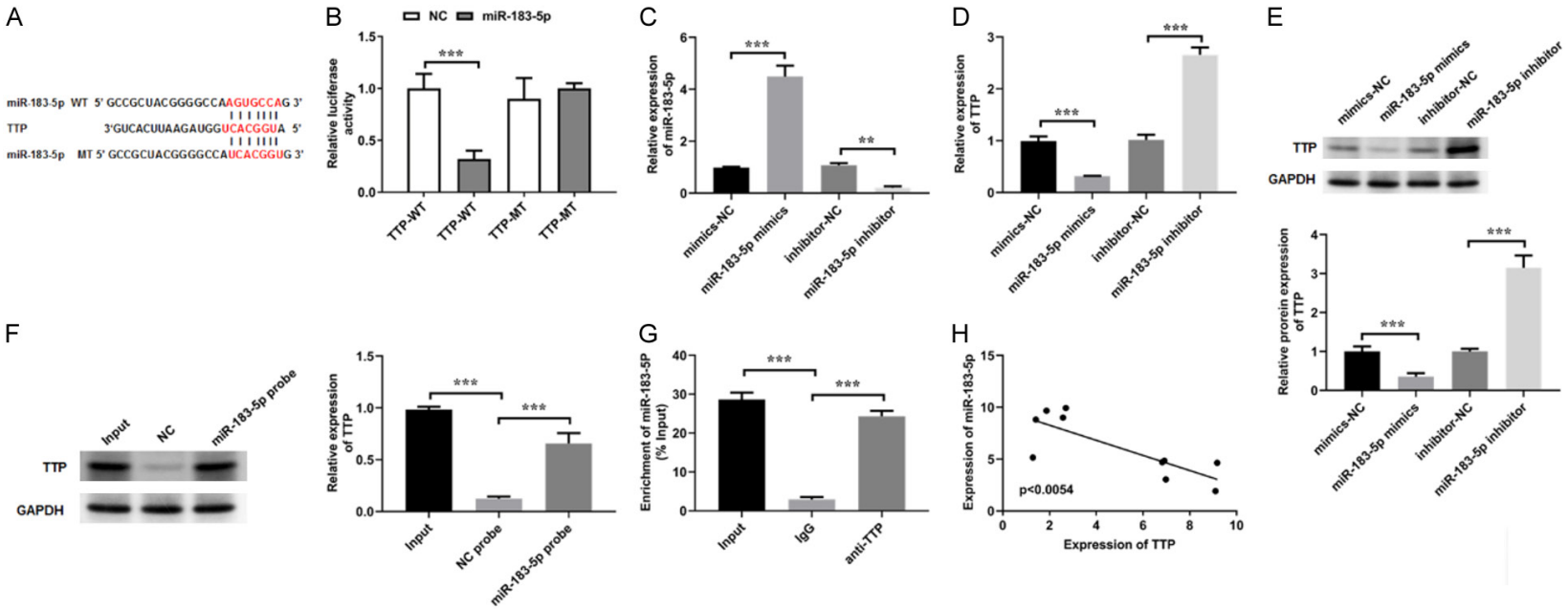

Figure 5. TTP was identified as the target gene of miR-183-5p. A. The binding sites of miR-183-5p and TTP; B. Dual luciferase reporter gene demonstrated the binding of miR-183-5p to TTP; C. The expression of miR-183-5p after various treatment; D, E. The expression of TTP after various treatment; F. The interaction of miR-183-5p with TTP RNA verified by RNA pull-down assay; G. The expression of miR-183-5p enriched with TTP antibodies detected by RIP; H. Correlation analysis of serum miR-183-5p and TTP in patients with DN. **P < 0.01, ***P < 0.001. TTP: tristetraprolin.

their mechanism of action, we co-transfected the TTP plasmid and miR-183-5p mimics into HK-2 cells. Results demonstrated that the TTP overexpression plasmid effectively increased TTP expression in HK-2 cells, while the miR-183-5p mimics significantly reduced TTP levels (**Figure 6A**). Cell proliferation assays revealed that TTP overexpression stimulated HK-2 cell proliferation, whereas the miR-183-5p mimic hindered HK-2 cell proliferation, and TTP overexpression reversed the proliferation inhibition caused by miR-183-5p (**Figure 6B**). Analysis of IL-6 and TNF-α expression revealed that TTP overexpression significantly reduced the levels of IL-6 and TNF-α, whereas the miR-183-5p mimics upregulated the levels of both cytokines (**Figure 6C**, **6D**). Apoptosis assays revealed that miR-183-5p mimics enhanced the apoptosis of HK-2 cells, and TTP overexpression counteracted the pro-apoptosis effects of miR-183-5p (**Figure 6E**). Analysis of apoptosis-associated molecules revealed that TTP overexpression inhibited Bax, while miR-183-5p mimics promoted Bax expression, and TTP could reverse the pro-apoptotic influence induced by miR-183-5p mimics (**Figure 6F**). The variation trend of Bcl-2 expression was opposite to that of Bax (**Figure 6G**).

Knockdown of miR-183-5p attenuated renal inflammation and apoptosis in db/db mice

Increased miR-183-5p expression and decreased TTP expression were observed in the kidney tissues of db/db mice. Administration of a miR-183-5p inhibitor effectively downregulated miR-183-5p levels (Supplementary Figure 4A) and upregulated TTP expression (Supplementary Figure 4B). TUNEL staining revealed elevated apoptosis in the kidneys of db/db mice, which was significantly reduced upon inhibition of miR-183-5p (Supplementary Figure 4C). Additionally, increased IL-6 secretion (Supplementary Figure 4D) and reduced Bcl-2 expression (Supplementary Figure 4E) were observed in the kidney tissues of db/db mouse; miR-183-5p inhibitor attenuated inflammatory cytokine production and enhanced expression of the anti-apoptotic protein Bcl-2. Histological analysis by H&E staining showed normal glomerular and tubular architecture with no apparent mesangial matrix expansion or sclerosis in control mice. In contrast, db/db mice displayed coexisting glomerular hypertrophy and atrophy accompanied by mesangial matrix accumulation, along with tubular vacuolization. Notably, treatment with the miR-183-5p inhibitor markedly ameliorated these pathological changes and alleviated renal injury (Supplementary Figure 4F).

Discussion

The development of diabetic nephropathy (DN) involves the combined effects of multiple factors, including alterations in renal hemodynamics, oxidative stress, and cytokines, all of which contribute significantly to disease progression [16, 17]. Studies using microarray technology, Dicer gene knockout, and various *in vivo* and *in vitro* experiments indicate that miRNA exert differential effects on different cell types in DN. Therefore, the molecular interaction mechanisms between miRNA and DN warrant further in-depth investigation. Gaining a thorough understanding of the targets of relevant miRNA can provide novel insights for the early diagnosis and management of DN.

Inflammatory and immune responses also play pivotal roles in the development and progression of DN. Inflammatory mediators (e.g., TNF-α, monocyte chemoattractant protein (MCP-1)) and immune cells (e.g., Th1 and Th17) are all closely associated with DN development. Research on diabetic mice have demonstrated that overexpression of miRNA-29b attenuates renal fibrosis and inflammation, while miRNA-29b knockout exacerbates these response [18]. As a key signaling pathway in DN, the NF-κB pathway participates in multiple biological processes including immune responses and apoptosis. Its activation leads to upregulation of pro-inflammatory factors like TNF-α and MCP-1, promoting macrophage infiltration [19]. Our experimental results indicate that overexpression of miR-183-5p in renal tubular epithelial cells increases inflammatory cytokine levels, whereas inhibition of miR-183-5p reduces inflammatory markers in tubular cells. Existing evidence supports the potential pro-inflammatory role of miR-183-5p in the development and progression of DN.

TTP regulates various inflammatory cytokines, transcription factors, and inflammatory chemokines, including TNF-α, IL-2, IL-6 and VEGF, and contributes to the progression of inflammation [20-22]. Via both in vitro assays and in vivo studies, It is reported that TTP in vascular endo-

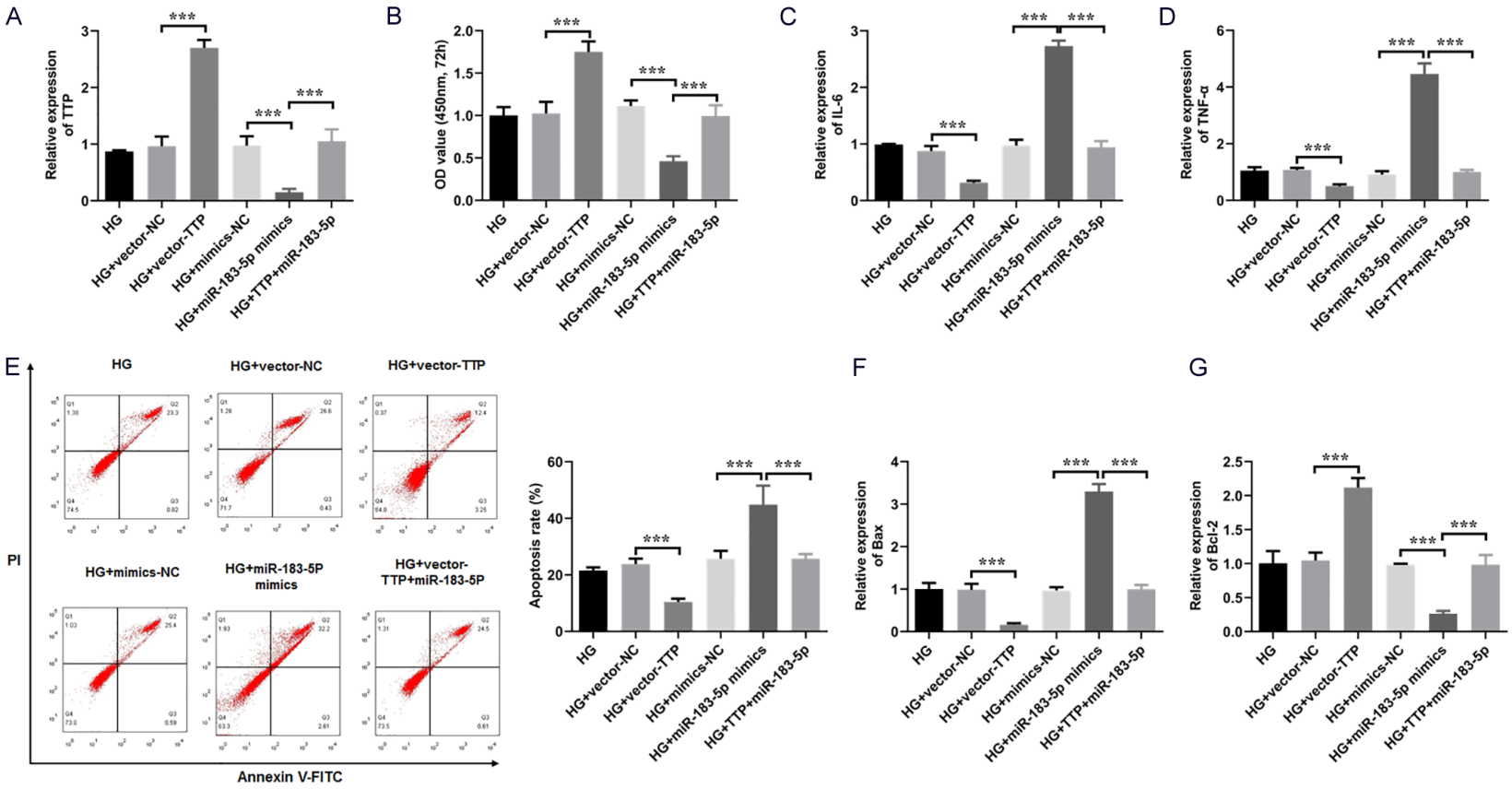

Figure 6. TTP overexpression reversed the pro-inflammation and pro-apoptosis effects induced by miR-183-5p. A. Detection of TTP expression. B. Detection of cell proliferation. C. Detection of IL-6 expression after different treatments. D. Detection of TNF-α expression after different treatments. E. Apoptosis was detected by flow cytometry after different treatments. F. Detection of apoptotic protein Bax after different treatments. G. Detection of anti-apoptotic protein Bcl-2 after different treatments. ***P < 0.001. TTP: tristetraprolin; IL-6: interleukin-6; TNF-α: tumor necrosis factor-alpha; Bax: Bcl-2-associated X protein; Bcl-2: B-cell lymphoma 2.

thelial cells and macrophages can suppress the generation of proinflammatory cytokine mRNA and enhance the concentration of TTP in blood vessels, which can reduce the occurrence of vascular inflammation [23]. In addition, the TTP gene is located in the long arm of chromosome of 19q13.1, which is closely related to metabolic syndrome. It has been reported that the polymorphism of the TTP gene in obese patients is closely related to body mass index, fasting blood glucose and LDL-C, and the TTP gene may be an important gene related to the obesity-related complications of metabolic syndrome [24, 25].

Our findings demonstrate that under hyperglycemia conditions, miR-183-5p specifically binds to TTP and promotes inflammatory and apoptotic responses. Prior reports have highlighted that miRNAs serve as key biomarkers for diverse complex diseases, including DN. Therefore, identifying crucial miRNAs in DN and objectively evaluating their expression are crucial for the early diagnosis and management of this condition. To this end, we measured miRNA expression levels in plasma in patients with T2DM, DN, and healthy controls. Results showed that plasma miR-183-5p levels were significantly elevated in patients with T2DM and DN, consistent with the findings reported [26]. However, the underlying reasons for the differential expression of miR-183-5p remain unclear and may be related to the pathophysiological response of hyperglycemia.

The hypertonic state can activate multiple cellular stress pathways, inducing oxidative stress, inflammatory responses, and apoptosis, which may interfere with the accurate assessment of glucose-specific biological effects. To eliminate this potential confounding factor, we added an isotonic mannitol control group (5.5 mM glucose + 19.5 mM mannitol) in the key experiments, ensuring its osmotic pressure level matched that of the high glucose group. Results showed that compared with the normal glucose group (NG), the mannitol group (MG) exhibited a slightly yet insignificant increased trend of inflammatory factors and apoptosis. In contrast, the HG group demonstrated a significantly pronounced upregulation in both inflammatory marker expression and apoptosis. These findings suggest that the observed upregulation of miR-183-5p, downregulation of TTP, and significant enhancement of inflammation and apoptosis are mainly attributed to the metabolic effect of high-concentration glucose rather than simple changes in osmotic pressure.

Conclusion

miR-183-5p contributes to the inflammatory response triggered by hyperglycemia and promotes DN development through its action on TTP. These results offer new insights into the role of miR-183-5p in the diabetic milieu and pave the way for new therapeutic approaches for DN management.

Limitations

Although 25 mM glucose does increase osmotic pressure compared to normal glucose conditions (typically 5.5 mM), this concentration is commonly used in the literature to simulate chronic hyperglycemia *in vitro*. Furthermore, many studies employ low-glucose or normal-glucose controls as baselines. Therefore, the lack of osmolarity control is a limitation of this study, which will be addressed in subsequent experiments. Another limitation is the small clinical sample size with only a preliminary finding to determine potential differences in specific biomarkers. While the current findings represent preliminary observations aimed at identifying potential differences in specific biomarkers, future research will expand the clinical sample size to further validate these conclusions.

Acknowledgements

This study was supported by the Elderly Health Research Project of Jiangsu Province (No. LKM2024040).

Disclosure of conflict of interest

None.

Address correspondence to: Yan Gu, Department of Geriatric Medicine, Nantong First People's Hospital, No. 666 Shengli Road, Nantong 226000, Jiangsu, China. E-mail: ntguyan1980@ntu.edu.cn

References

[1] Dwivedi S and Sikarwar MS. Diabetic nephropathy: pathogenesis, mechanisms, and therapeutic strategies. Horm Metab Res 2025; 57: 7-17.

[2] Samsu N. Diabetic nephropathy: challenges in pathogenesis, diagnosis, and treatment. Biomed Res Int 2021; 2021: 1497449.
[3] Li X, Lu L, Hou W, Huang T, Chen X, Qi J, Zhao Y and Zhu M. Epigenetics in the pathogenesis of diabetic nephropathy. Acta Biochim Biophys Sin (Shanghai) 2022; 54: 163-172.
[4] Thomas S and Karalliedde J. Diabetic nephropathy. Medicine 2019.
[5] Shima K, Hirota M, Fukuda M and Tanaka A. Determination of urinary lysozyme for potential detection of tubular dysfunction in diabetic nephropathy. Clin Chem 1986; 32: 1818-22.
[6] Zhang Y, Le X, Zheng S, Zhang K, He J, Liu M, Tu C, Rao W, Du H, Ouyang Y, Li C and Wu D. MicroRNA-146a-5p-modified human umbilical cord mesenchymal stem cells enhance protection against diabetic nephropathy in rats through facilitating M2 macrophage polarization. Stem Cell Res Ther 2022; 13: 171.
[7] Szostak J, Gorący A, Durys D, Dec P, Modrzejewski A and Pawlik A. The role of MicroRNA in the pathogenesis of diabetic nephropathy. Int J Mol Sci 2023; 24: 6214.
[8] Abdelmaksoud NM, Al-Noshokaty TM, Abdelhamid R, Abdellatif N, Mansour A, Mohamed R, Mohamed AH, Khalil NAE, Abdelhamid SS, Mohsen A, Abdelaal H, Tawfik A and Elshaer SS. Deciphering the role of MicroRNAs in diabetic nephropathy: regulatory mechanisms and molecular insights. Pathol Res Pract 2024; 256: 155237.
[9] Kaur P, Kotru S, Singh S and Munshi A. miRNA signatures in diabetic retinopathy and nephropathy: delineating underlying mechanisms. J Physiol Biochem 2022; 78: 19-37.
[10] Hu S, Yan J, Yuan Q, Meng T, Cai Z, Huang Y and Wang Y. The role of miRNAs in podocyte injury in diabetic nephropathy: mechanisms and clinical applications. Curr Mol Pharmacol 2024; 17: e18761429363169.
[11] Noei Razliqi R, Ahangarpour A, Mard SA and Khorsandi L. Gentisic acid protects against diabetic nephropathy in nicotinamide-streptozotocin administered male mice by attenuating oxidative stress and inflammation: the role of miR-200a/Keap1/Nrf2 pathway, renin-angiotensin system (RAS) and NF-κB. Chem Biol Interact 2023; 380: 110507.
[12] Niu Z, Ren G, Huang L and Mu L. Circ_0008529 contributes to renal tubular cell dysfunction in high glucose stress via miR-185-5p/SMAD2 pathway in diabetic nephropathy. Biochem Genet 2023; 61: 963-978.
[13] Aboismaiel MG, Amin MN and Eissa LA. Renoprotective effect of a novel combination of 6-gingerol and metformin in high-fat diet/streptozotocin-induced diabetic nephropathy in rats via targeting miRNA-146a, miRNA-223, TLR4/TRAF6/NLRP3 inflammasome pathway and HIF-1α. Biol Res 2024; 57: 47.
[14] Snyder BL and Blackshear PJ. Clinical implications of tristetraprolin (TTP) modulation in the treatment of inflammatory diseases. Pharmacol Ther 2022; 239: 108198.
[15] Rezcallah MC, Al-Mazi T and Ammit AJ. Cataloguing the phosphorylation sites of tristetraprolin (TTP): functional implications for inflammatory diseases. Cell Signal 2021; 78: 109868.
[16] Ma L, Wu F, Shao Q, Chen G, Xu L and Lu F. Baicalin alleviates oxidative stress and inflammation in diabetic nephropathy via Nrf2 and MAPK signaling pathway. Drug Des Devel Ther 2021; 15: 3207-3221.
[17] Rayego-Mateos S, Morgado-Pascual JL, Opazo-Ríos L, Guerrero-Hue M, García-Caballero C, Vázquez-Carballo C, Mas S, Sanz AB, Herencia C, Mezzano S, Gómez-Guerrero C, Moreno JA and Egido J. Pathogenic pathways and therapeutic approaches targeting inflammation in diabetic nephropathy. Int J Mol Sci 2020; 21: 3798.
[18] Liu J, Xiong Y, Mo H, Niu H, Miao J, Shen W, Zhou S, Wang X, Li X, Zhang Y, Ma K and Zhou L. MicroRNA-29b plays a vital role in podocyte injury and glomerular diseases through inducing mitochondrial dysfunction. Int J Biol Sci 2024; 20: 4654-4673.
[19] Qiu D, Song S, Chen N, Bian Y, Yuan C, Zhang W, Duan H and Shi Y. NQO1 alleviates renal fibrosis by inhibiting the TLR4/NF-κB and TGF-β/Smad signaling pathways in diabetic nephropathy. Cell Signal 2023; 108: 110712.
[20] Cook ME, Bradstreet TR, Webber AM, Kim J, Santeford A, Harris KM, Murphy MK, Tran J, Abdalla NM, Schwarzkopf EA, Greco SC, Halabi CM, Apte RS, Blackshear PJ and Edelson BT. The ZFP36 family of RNA binding proteins regulates homeostatic and autoreactive T cell responses. Sci Immunol 2022; 7: eabo0981.
[21] Wang Y, Zhao S Y, Wang Y C, Xu J and Wang J. The immune-inflammation factor is associated with diabetic nephropathy: evidence from NHANES 2013-2018 and GEO database. Sci Rep 2024; 14: 17760.
[22] Uehara Y, Suzukawa M, Horie M, Igarashi S, Minegishi M, Takada K, Saito A and Nagase H. ZFP36 family expression is suppressed by Th2 cells in asthma, leading to enhanced synthesis of inflammatory cytokines and cell surface molecules. Cell Immunol 2024; 403-404: 104859.
[23] Wu L, Feng M, Peng Y, Xiang Y, Liu R and Liu T. Study on the efficacy and mechanism of metabolomics and bioinformatics on the treatment of Qi stagnation and blood stasis coro-

nary heart disease by danshen injection. Biomed Chromatogr 2025; 39: e70120.
[24] Hu Y, Hai J, Ti Y, Kong B, Yao G, Zhao Y, Zhang C, Zheng X, Zhang C, Ma X, Yu H, Qin X, Kovarik P, Zhang C, Liu S, Zhang W, Li J and Bu P. Adipose ZFP36 protects against diet-induced obesity and insulin resistance. Metabolism 2025; 164: 156131.
[25] Louis J M, Agarwal A, Aduri R and Talukdar I. Global analysis of RNA-protein interactions in TNF-α induced alternative splicing in metabolic disorders. FEBS Lett 2021; 595: 476-490.
[26] Asadi G, Rezaei Varmaziar F, Karimi M, Rajabinejad M, Ranjbar S, Gorgin Karaji A, Salari F, Afshar Hezarkhani L and Rezaiemanesh A. Determination of the transcriptional level of long non-coding RNA NEAT-1, downstream target microRNAs, and genes targeted by microRNAs in diabetic neuropathy patients. Immunol Lett 2021; 232: 20-26.

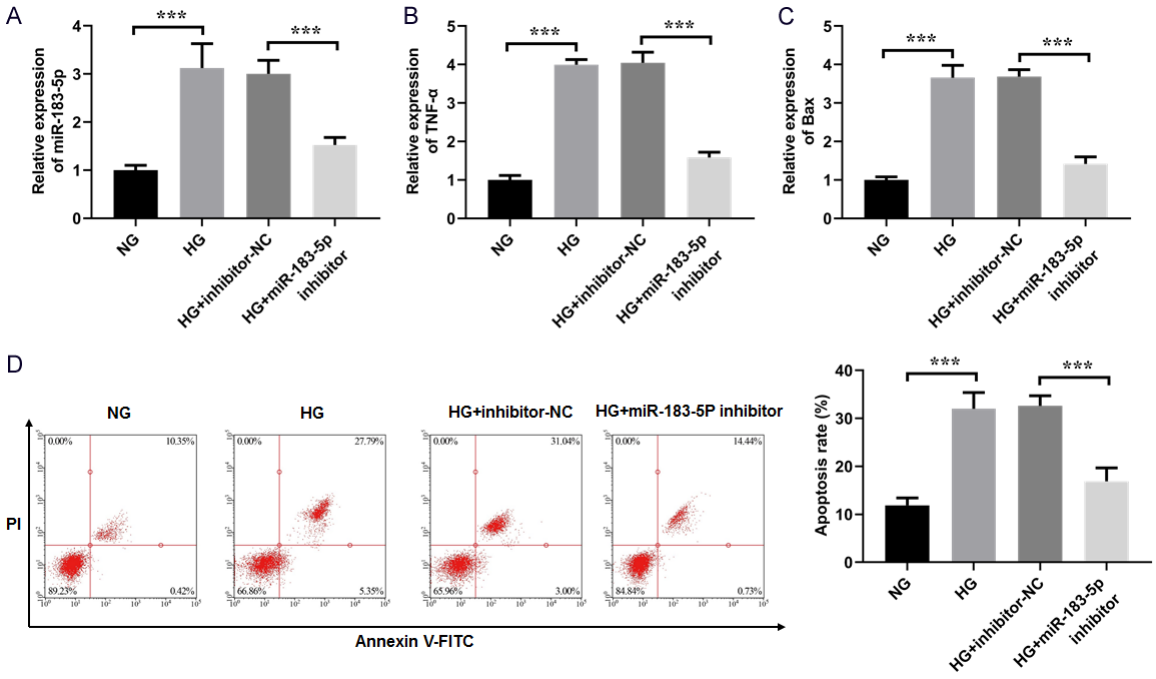

Supplementary Figure 1. Inhibition of miR-183-5p alleviated inflammation and apoptosis in HG treated HRMMCs. A. miR-183-5p expression was detected after various treatment; B. TNF-α expression was detected after various treatment; C. mRNA expression of Bax. D. Apoptosis of HRMMCs detected by flow cytometry. ***P < 0.001. TNF-α: tumor necrosis factor-alpha; Bax: Bcl-2-associated X protein.

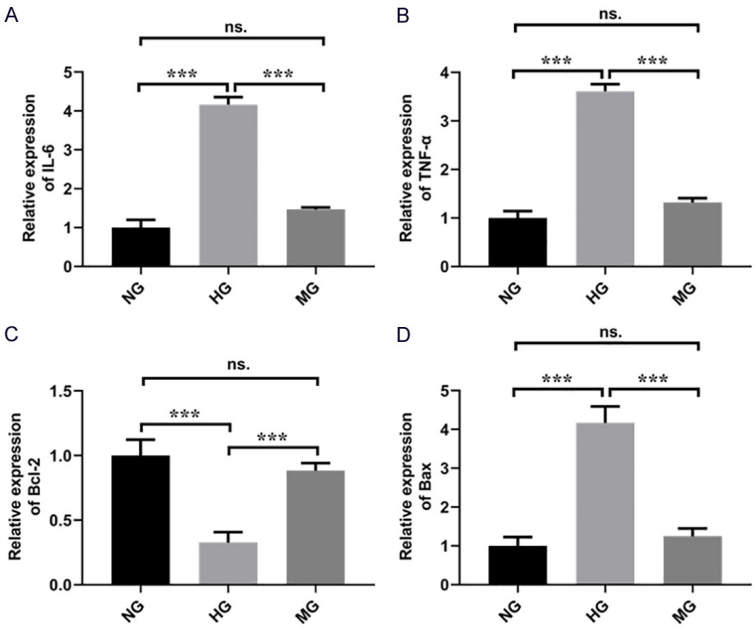

Supplementary Figure 2. The effect of osmotic pressure on inflammation and apoptosis. A. IL-6 expression; B. TNF-α expression; C. Bcl-2 expression; D. Bax expression. *P < 0.05, **P < 0.01, ***P < 0.001. HG: high glucose group. MG: mannitol group. NG: normal glucose. IL-6: interleukin-6; TNF-α: tumor necrosis factor-alpha; Bax: Bcl-2-associated X protein; Bcl-2: B-cell lymphoma 2.

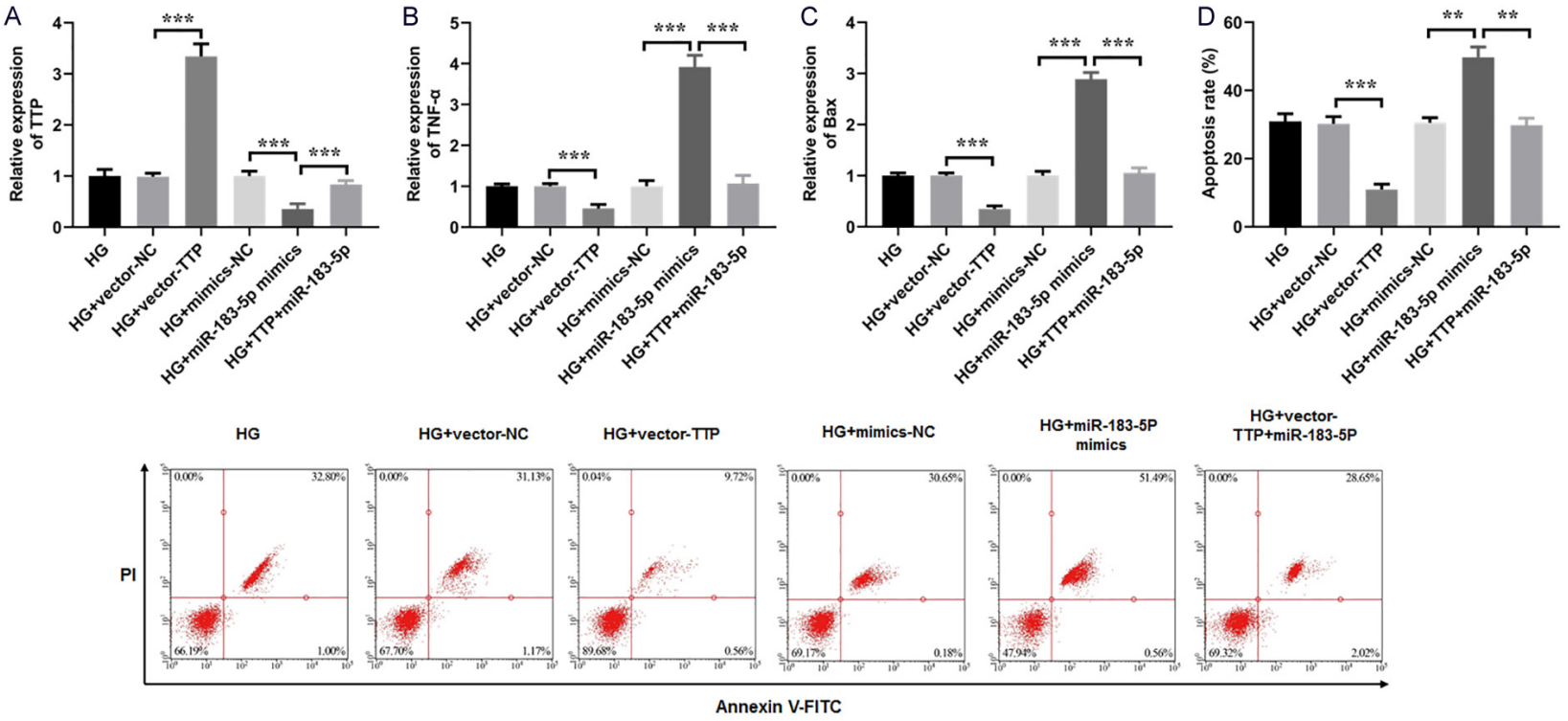

Supplementary Figure 3. MiR-183-5p promoted inflammation and apoptosis in HG treated HRGMCs by upregulating TTP. A. TTP expression. B. TNF-α expression. C. Bax expression. D. Apoptosis. **P < 0.01, ***P < 0.001. TTP: tristetraprolin; TNF-α: tumor necrosis factor-alpha; Bax: Bcl-2-associated X protein.

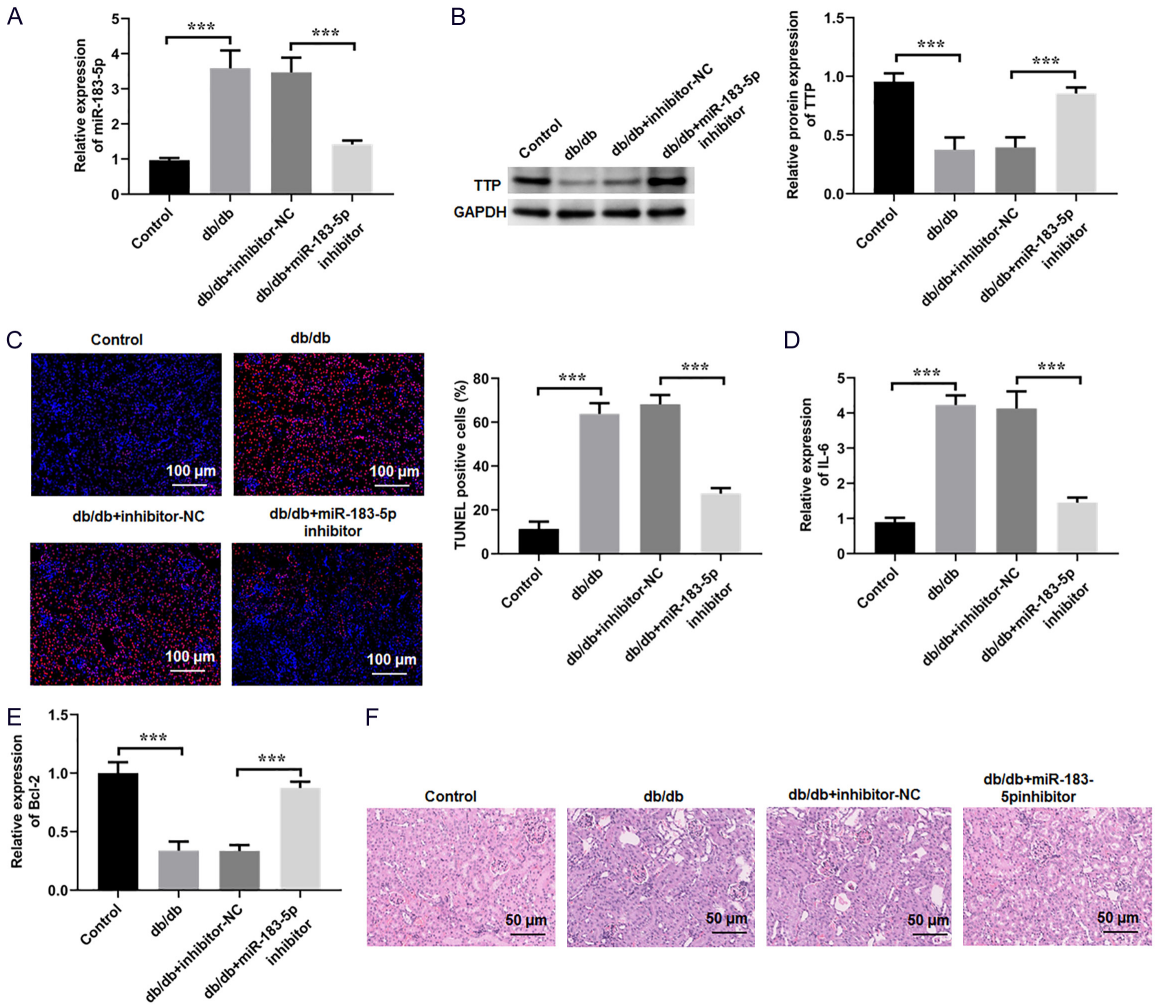

Supplementary Figure 4. Inhibition of miR-183-5p expression alleviated renal damage in db/db mice. A. miR-183-5p expression; B. TTP expression; C. Apoptosis detected by TUNEL assay; Scale = 100 μm; D. IL-6 expression; E. Bcl-2 expression; F. Representative image of HE staining of renal tissue. Scale = 50 μm. ***P < 0.001. TTP: tristetraprolin; IL-6: interleukin-6; Bcl-2: B-cell lymphoma 2.